

THE PERFORMANCE OF InGaN LASER DIODE CONSISTING OF A SEPARATE CONFINEMENT HETEROSTRUCTURE WITH A MULTIPLE QUANTUM WELL ACTIVE REGION

S. M. Thahab, H. Abu Hassan, Z. Hassan

Nano-Optoelectronics Research and Technology Laboratory
School of Physics, Universiti Sains Malaysia
11800 Penang, Malaysia

ABSTRACT

Low threshold operation of laser diodes depends on the confinement of the injected carriers to the active region. In this study InGaN multi-quantum wells (MQWs) laser diode with modulation doped strained layer superlattices (MD-SLS) as cladding layers and separate confinement heterostructure (SCH) confinement layers was simulated and investigated using ISE-TCAD software simulation program. The optical and electrical properties exhibited significant enhancement as compared to that in InGaN laser diode with bulk AlGaIn cladding layers. Output powers of 73 mW with threshold current of 18.2 mA were obtained. The internal quantum efficiency, laser diode far-field, and the transparency threshold current density were also calculated.

INTRODUCTION

InGaN-based laser diodes have potential in a number of applications such as optical storage, printing, full-color displays, chemical sensors, and medical applications. Major developments in recent years have led to demonstration of lifetimes in excess of 10 000 hours [1] and subsequent commercialization of nitride laser diodes [2]. The implementations of AlGaIn/GaN modulation-doped strained-layer superlattices and lateral epitaxial overgrowth in the laser structure have led to the increased lifetimes [3]. The reliability of these devices was further improved by using low-dislocation density free-standing GaN substrates [4]. Even with the commercialization of nitride lasers a reality, there is a continued drive to improve efficiency and operating characteristics. A thin AlGaIn cap is commonly inserted above the multiple quantum wells MQWs of InGaIn-based lasers and light-emitting diodes to prevent electron overflow from the active region and to protect the InGaIn active region from the high temperature growth of subsequent *p*-type layers [5].

Recombination of carriers outside of the wells reduces the internal quantum efficiency of the lasers. Electron overflow can be a serious problem in the nitrides because of poor hole injection due to low hole mobility and the high threshold carrier density required for lasing [6]. Low threshold operation of laser diodes depends on confinement of the injected carriers to the active region.

In this study we introduce laser diode structure with MD-SLS as cladding layers and

SCH as confinement layers. The electronic and optical properties of our laser diode structure have been characterized using the ISE-TCAD [7].

Laser Structure and Parameters used in the Numerical Simulations

The laser simulation program [7, 8] solved the Poisson equation, the current continuity equations, the photon rate equation and the scalar wave equation using the two-dimensional (2-D) simulator. The carrier drift-diffusion model which includes Fermi statistics and incomplete ionization were included in our simulation models.

The Shockley Read–Hall (SRH) recombination lifetime of electrons and holes is assumed to be 1 ns; however, this is a rough estimate since the type and density of recombination centers are sensitive to the technological process. From its band gap dependence in other materials, a very small Auger parameter of $C = 1 \times 10^{-34} \text{ cm}^6 \text{ s}^{-1}$ is estimated for GaN. Thus, even with large carrier densities, Auger recombination in nitride materials is negligible. In our strained InGaN quantum wells GaN values are used for the deformation potentials.

n-type GaN layer that is 3 μm in thickness is assumed to grow first then followed by 80 pairs of (2.5 nm) n-type $\text{Al}_{0.1}\text{Ga}_{0.9}\text{N}/(2.5\text{nm})$ n-GaN MD-SLS layers, followed by a 0.1 μm n-type GaN guiding layer. 20 nm of n- $\text{Al}_{0.10}\text{Ga}_{0.90}\text{N}$ (SCH) is assumed to grow after n-GaN guided layer. The active region of the preliminary laser diode structure under study consists of a 3 nm $\text{In}_{0.13}\text{Ga}_{0.87}\text{N}$ well that is sandwiched between two 5 nm $\text{In}_{0.01}\text{Ga}_{0.99}\text{N}$ barriers. 0.005 μm p- $\text{Al}_{0.15}\text{Ga}_{0.85}\text{N}$ stopper layer is assumed to be grown on the top of the active region, followed by 0.1 μm p-type GaN guiding layer, followed by 80 pairs of (2.5nm) p-type $\text{Al}_{0.1}\text{Ga}_{0.9}\text{N}/(2.5 \text{ nm})$ p-GaN MD-SLS layers p and 0.1 μm p-GaN contact layer. The doping concentration of n-type and p-type are $5 \times 10^{17} \text{ cm}^{-3}$ and $5 \times 10^{18} \text{ cm}^{-3}$ respectively. The laser cavity region length is 800 μm and width 1 μm . The reflectivities of the two ends of left and right facets are both set at 30%.

RESULTS AND DISCUSSION

For our InGaN laser diode under study, Figure 1 shows the overall energy band gap diagram of the DQWs MD-SLS. It can be seen that the $\text{In}_{0.13} \text{Ga}_{0.87}\text{N}$ wells have lower bandgap compare to that in the $\text{Al}_{0.15}\text{Ga}_{0.85}\text{N}$ stopper layer and GaN waveguide layers. This will allow more carriers to accumulate in the active region and enhance the carrier recombination rate.

The electron leakage current is larger than the hole leakage current due to the usually larger diffusion constant of electrons compared with holes in III-V semiconductor. To reduce carrier leakage out of the active region, carrier –stopper layers are used. Such electron stoppers are regions with high band gap energy located at the confinement-active interface. It is found that the AlGaN stopper layer plays a role in avoiding the electron leakage. The carriers confinement was achieved by the SCH producing high radiative recombination rate inside the active region, which consequently, produces high optical gain and output power.

Figure 2 shows the valence band and the conduction band profile of MD-SLS InGaN DQW LD. The right side of the diagram is the n-side and the left side is the p-side of the laser diode, the horizontal axis is the distance along the crystal growth direction. It can be seen that the superlattices produce the necessary valence band edge oscillation by employing alloys with different valence band edge positions. The optical intensity together with the refractive index profile is shown in Figure 3. Maximum optical intensity was observed at the laser diode active region due to the higher optical confinement achieved by the refractive index profile provided by the GaN waveguide and AlGaN/GaN MD-SLS cladding layer.

Output power of 73mW with threshold current of 18.2 mA is obtained with turn-on voltage of 3 V at a laser bias voltage of 7.5 V as shown in Figure 4. The laser diode transparency current density (J_0) is the current that provides just sufficient injection to lead stimulated emission just balancing absorption. In order to obtain the J_0 value, the curve of threshold current density versus the inverse cavity length is plotted as shown in Figure 5. The intercept of the linear fit line of the data plotted in this curve with the vertical axis provides us with the J_0 value.

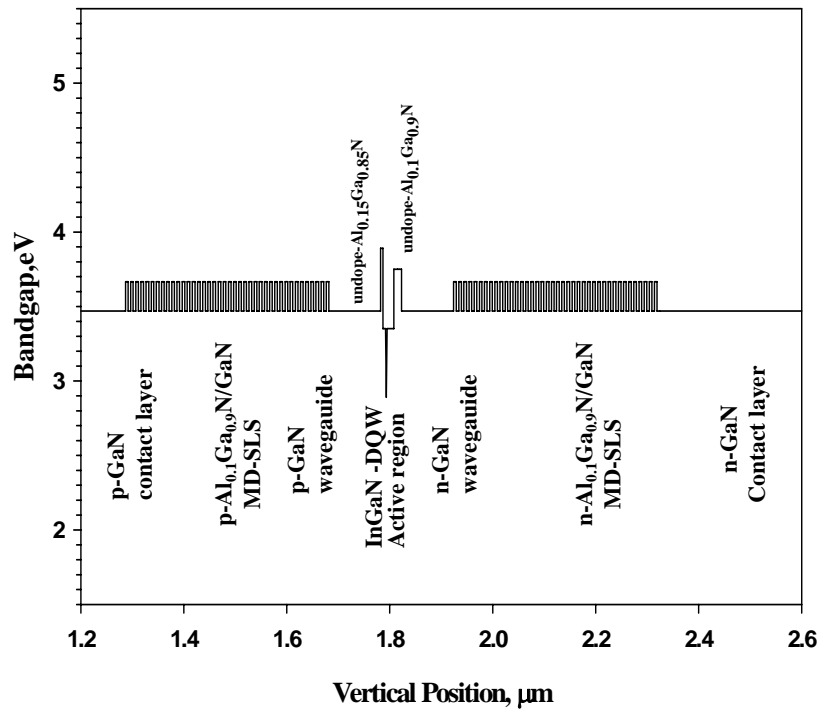


Figure 1: Bandgap energy profile of MD-SLS InGaN DQWs LD

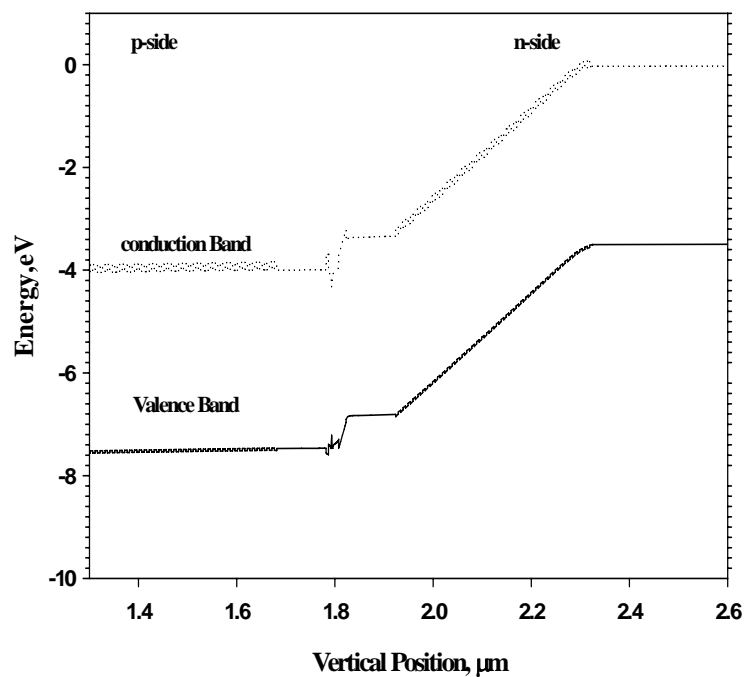


Figure 2: valence band and the conduction band profile of MD-SLS InGaN DQW LD.

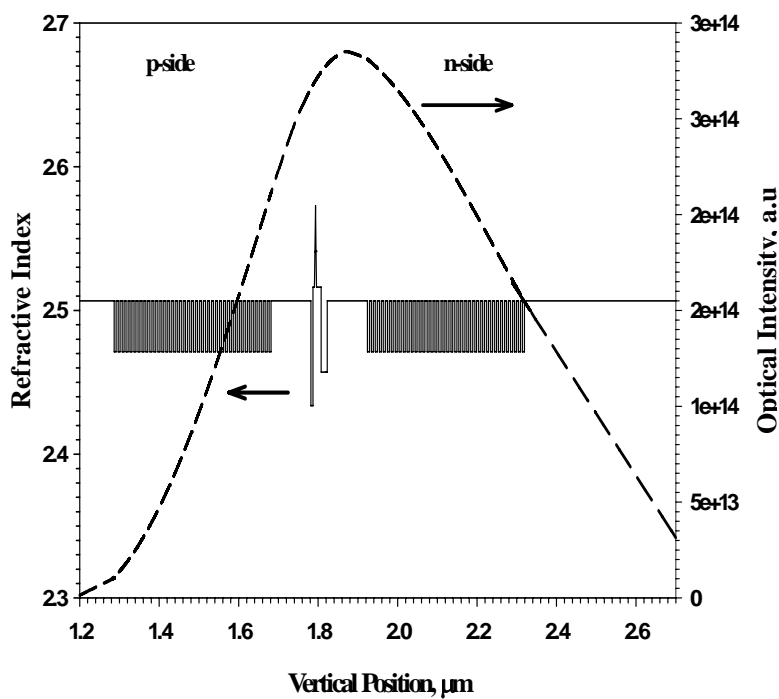


Figure 3: The optical intensity and the refractive index profile of the MD-SLS InGaN DQW.

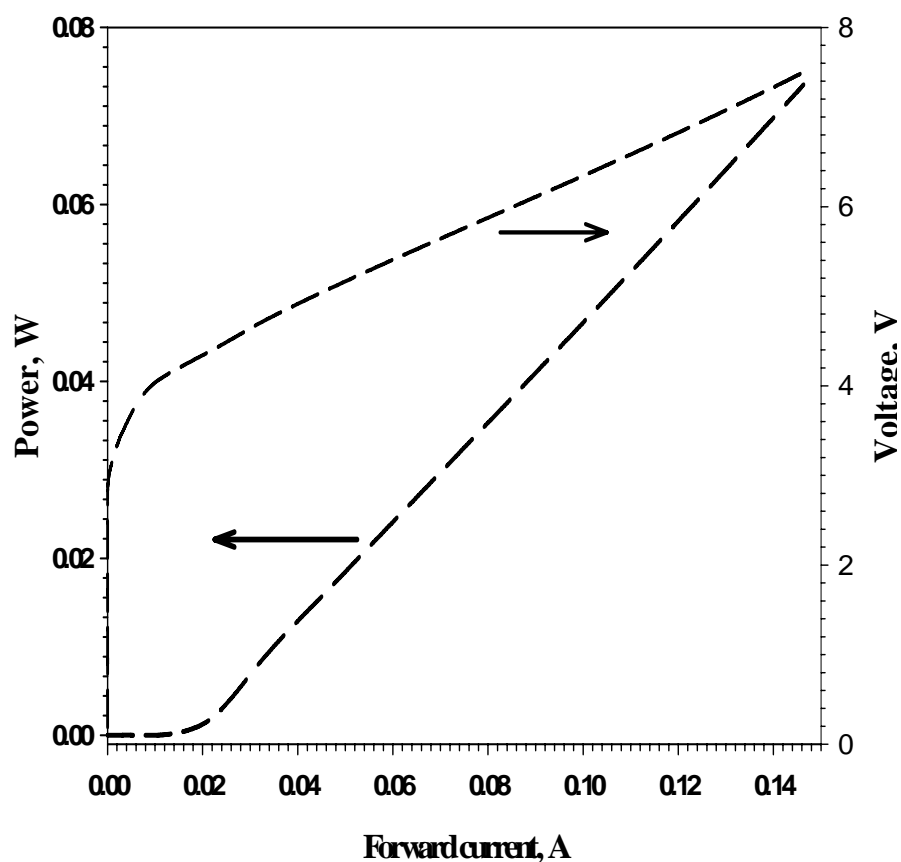


Figure 4: The output power and bias voltage of MD-SLS InGaN DQW LD as a function forward current.

It is observed that the InGaN DQWs laser diode with MD-SLS has a lower J_0 value of 680.9 A/cm^2 . This indicates that the lasing in InGaN laser diode with MD-SLS could be achieved at a lower threshold current density.

The far-field pattern of a semiconductor laser diode is the proper collection of the radiative power. It is also a measure of the waveguiding properties which give a reality check on the calculation of the field distribution, the validity of the composition, the doping and also the temperature.

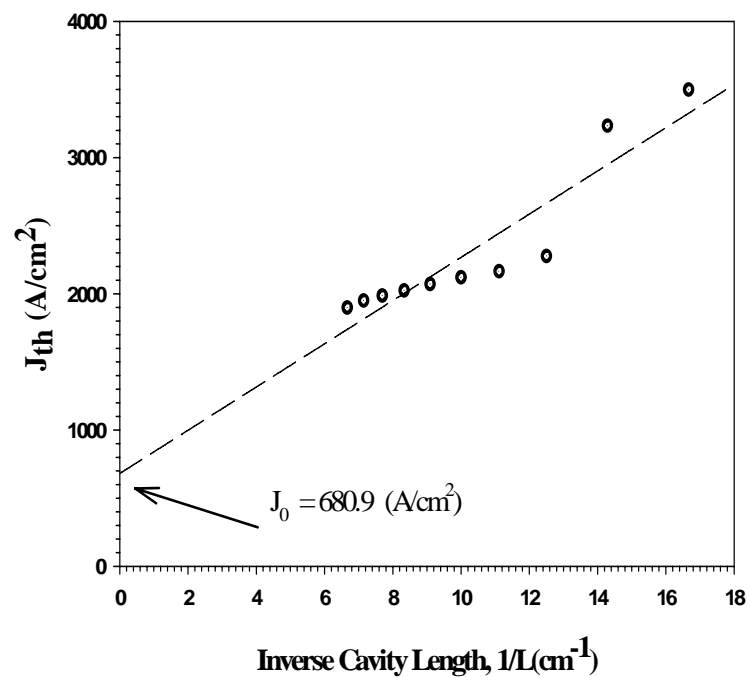


Figure 5: The threshold current density as a function of inverse cavity length of MD-SLS DQW InGaN

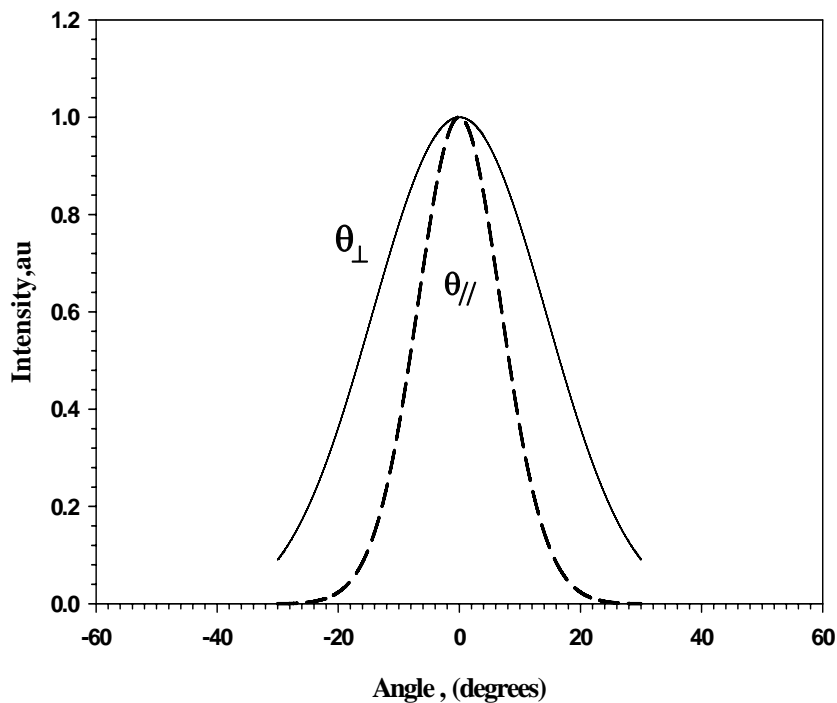


Figure 6: The Far-Filed pattern of MD-SLS DQW InGaN LD.

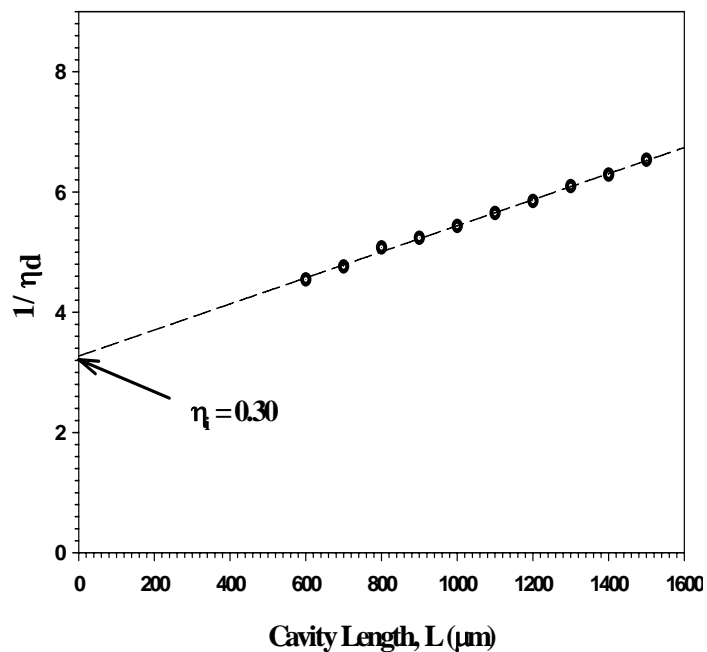


Figure 7: Inverse of the DQE as a function of cavity length of MD-SLS InGaN DQW LD.

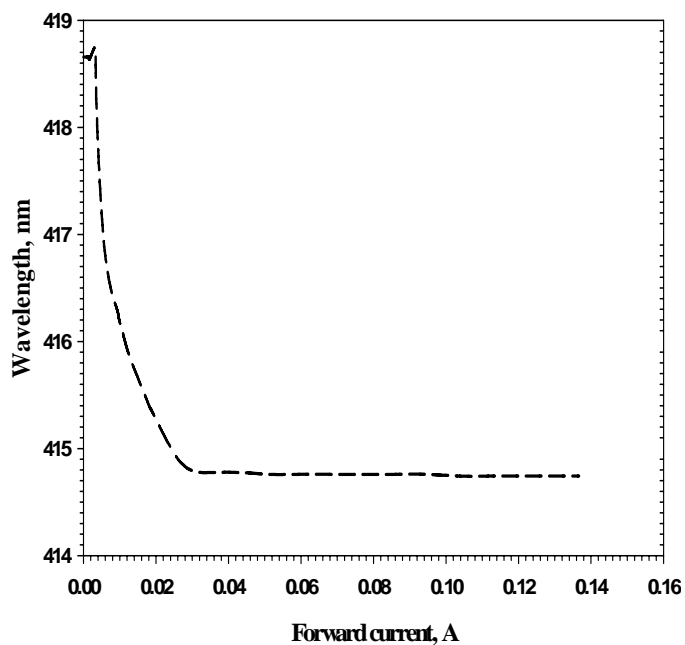


Figure 8: Output wavelength of MD-SLS InGaN DQW LD as a function of forward current.

The radiative pattern emanating from our MD-SLS laser diode is shown in Figure 6, where $\theta_{//}$ and θ_{\perp} represent the full angle at half power in the directions parallel and perpendicular to the plan of junction respectively. The values of 16° and 32° are obtained for the FWHM $\theta_{//}$ and FWHM θ_{\perp} , respectively.

Internal quantum efficiency (η_i) can be determined from the vertical axis intercept point of the linear fit line produced by plotting the inverse external differential quantum efficiency (DQE) ($1/\eta_d$) versus cavity length (L). Figure 7 shows the calculation method of η_i with respect to inverse value of DQE as a function of the cavity length. A value of 30% for η_i is obtained. A blue shift of the emission wavelength from 418.7nm to 414.8 nm with an increase in the forward current has been observed as shown in Figure 8. Applying a forward bias reduces the electric field, thereby countering the quantum confined Stark effect (QCSE) in the active region.

CONCLUSION

MD-SLS InGaN LD consisting of SCH with MQW region has been investigated. The LD exhibited high performance with an output power of 73 mW and threshold current value of 18.2 m A. The carriers confinement achieved by the SCH produced high radiative recombination rates inside the active region, which consequently, produces high optical gain and output power. The MD-SLS InGaN SCH DQW LD exhibited reliable performance that is reflected from the characterized parameters such as J_0 and η_i calculated in this work.

ACKNOWLEDGMENTS

Supports from Universiti Sains Malaysia and Ministry of Science, Technology and Innovation are gratefully acknowledged.

REFERENCES

- [1]. S. Nakamura, M. Senoh, S. Nagahama, N. Iwasa, T. Yamada, T. Matsushita, H. Kiyoku, Y. Sugimoto, T. Kozaki, H. Umemoto, M. Sano, and K. Chocho, (1997); *Proceedings of the International Conference on Nitride Semiconductors*, **S-1**, 444.
- [2]. S. Nakamura, (1999); *Proc. SPIE*, **158**, 3628
- [3]. S. Nakamura, M. Senoh, S. Nagahama, N. Iwasa, T. Yamada, T. Matsushita, H. Kiyoku, Y. Sugimoto, T. Kozaki, H. Umemoto, M. Sano, and K. Chocho, (1998); *Appl. Phys. Lett.* **72**, 211,
- [4]. S. Nagahama, N. Iwasa, M. Senoh, T. Matsushita, Y. Sugimoto, H. Kiyoku, T. Kozaki, M. Sano, H. Matsumura, H. Umemoto, K. Chocho, and T. Mukai, (2000);

Jpn. J. Appl. Phys. **39**, L647.

- [5]. S. Nakamura and G. Fasol, (1997); *The Blue Laser Diode*, Springer, Berlin.
- [6]. K. Domen, R. Soejima, A. Kuramata, and T. Tanahashi, (1998); *MRS Internet J.Nitride Semicond. Res.* **3**, 2.
- [7]. Integrated System Engineering (ISE TCAD) AG, Switzerland,
<http://www.synopsy.com>.
- [8]. S. M. Thahab, H. Abu Hassan, Z. Hassan, (2007); *Opt. Exp.*, **15**, No.5, 2380,